

Iterative Solution of Transonic Flows over Airfoils and Wings, Including Flows at Mach 1 * †

ANTONY JAMESON

1 Introduction

Transonic aerodynamics is the focus of strong interest at the present time because it is known to encompass one of the most efficient regimes of flight. While current transport aircraft operate just below the speed of sound, more radical aerodynamic designs, such as R. T. Jones' proposal for a yawed wing in [1], favor operation at low supersonic speeds in the range from Mach 1 to 1.3 (a regime in which the sonic boom should pose no serious problem). The hodograph method of generating a flow together with the corresponding boundary shape has been perfected by Bauer, Garabedian and Korn [2]. It now provides a flexible tool for the design of supercritical wing sections which produce shockfree flow at a specified speed and angle of attack. Since, however, it yields no information about the flow at off design conditions, and is restricted to two dimensions, it needs to be complemented by a method for calculating the flow over specified shapes in two and three dimensions throughout the desired range of speed and angle of attack. An accurate and reliable method would eliminate the need to rely on massive wind tunnel testing, and should lead to more rational designs. Following the initial success of Murman and Cole [3], substantial progress has recently been made in the development of finite difference methods for the calculation of transonic flows (cf. [4], [5], [6], [7]). These methods have generally been restricted, however, either to flows which are subsonic at infinity, or to small disturbance theories. The present paper describes a method using a new 'rotated' difference scheme, which is suitable for the calculation of both two- and three-dimensional flows without restriction on the speed at infinity, and which has been successfully applied to a variety of flows over airplane wings, including the case of flight at Mach 1.

The mathematical difficulties of the problem are associated primarily with the mixed hyperbolic and elliptic type of the equations and the presence of discontinuities. The computational method should be capable of predicting the location and strength of the shock waves, and if it is to be capable of distinguishing a good from a bad aerodynamic design, it should also provide an indication of the associated wave drag. In three-dimensional applications the rapid growth in the number of points in the computational lattice also excludes any method which is not rather economical in its use of the computer. In meeting these objectives the primary choices to be made concern first the most suitable formulation of the equations, second the construction of a favorable coordinate system, and third the development of a finite difference scheme which is stable, convergent, and also capable of accommodating the proper discontinuities.

Since we are concerned with flow at fairly low supersonic Mach numbers over efficient aerodynamic shapes, we may reasonably suppose that the shock waves are quite weak. A strong shock wave would cause boundary layer separation and buffeting, invalidating the analysis, and a design which led to the presence of a strong shock wave would in any case be unsuitable because of the accompanying drag rise and loss of lift. The error in

*The work for this paper was performed at the Courant Institute of Mathematical Science, New York University, and supported by NASA under Grant No. 33-016-167 and by the U.S. Atomic Energy Commission under Contract No. AT(11-1)-3077. Reproduction in whole or in part permitted for any purpose of the United States Government.

†Reprinted from COMMUNICATIONS ON PURE AND APPLIED MATHEMATICS, VOL. XXVII, 283-309 (1974)

ignoring changes in entropy through shock waves, and the resulting vorticity, should therefore be small, and we can expect to obtain a satisfactory approximation by using the transonic potential equation for irrotational flow instead of the full Euler equations. In the case of three-dimensional calculations, in particular, the replacement of five dependent variables (three velocity components, pressure, and energy) by a single velocity potential leads to important savings in machine time and memory.

When the boundaries are prescribed, the non-existence (cf. [8]) of smooth transonic solutions of the potential equation requires consideration of weak solutions (cf. [9]). The appropriate solutions admit discontinuities across which mass is conserved but momentum is not, so that a drag force appears. The method is thus able to predict the onset of wave drag. If, however, we do not impose a restriction on the type of jumps to be allowed corresponding to the entropy inequality, weak solutions of the potential equation are in general nonunique. The equation is invariant under reversal of the flow direction, so that a body with fore and aft symmetry, for example, admits both a solution with a compression shock, and a corresponding reversed flow solution with an expansion shock. To obtain uniqueness we must exclude discontinuous expansions. We ought, therefore, to restore in the numerical scheme the directional property which was removed by the exclusion of entropy from the equations. This indicates the need to ensure that the dominant terms of the truncation error represent an artificial viscosity.

It was first shown by Murman and Cole for the case of the small disturbance equations that the required artificial viscosity can be introduced in an effective and simple manner by using retarded difference formulas to represent derivatives in the streamwise direction at all points in the hyperbolic region. This leads to a simple implicit scheme which can be solved line by line advancing with the stream. Moreover, when the dominant truncation error is included, the resulting differential equation resembles the viscous transonic equation, which admits solutions with the approximate structure of a shock wave (cf. [10]). The difference equations exhibit similar behavior. Shock waves emerge in the course of the calculation as compression layers spread over a few mesh widths in which the artificial viscosity becomes the dominant term.

The method described in this paper is based on a similar principle, but no assumption about the direction of flow is made in constructing the difference scheme. Instead, the proper directional property is obtained by ‘rotating’ the difference scheme to conform with the local stream direction. This avoids the need to align one of the coordinates with the flow in the supersonic zone, a source of difficulty when this zone extends towards infinity at near sonic free stream Mach numbers. The rotated scheme is derived by rearranging the equations as if they were written in a streamline and normal coordinate system. In the hyperbolic region retarded difference formulas are then used for all contributions to the streamwise second derivative, producing a positive artificial viscosity correctly oriented with the stream.

The method described in this paper is based on a similar principle, but no assumption about the direction of flow is made in constructing the difference scheme. Instead, the proper directional property is obtained by ‘rotating’ the difference scheme to conform with the local stream direction. This avoids the need to align one of the coordinates with the flow in the supersonic zone, a source of difficulty when this zone extends towards infinity at near sonic free stream Mach numbers. The rotated scheme is derived by rearranging the equations as if they were written in a streamline and normal coordinate system. In the hyperbolic region retarded difference formulas are then used for all contributions to the streamwise second derivative, producing a positive artificial viscosity correctly oriented with the stream.

The method retains the property of the Murman scheme of automatically locating the shocks. This is a great advantage for the flows to be considered, which may contain a complex pattern of shocks above and below the wing, together with a detached bow shock if the flow is supersonic at infinity.

2 Formulation of the Equations

In the isentropic flow of a perfect gas the equation of state

$$(2.1) \quad \frac{p}{\rho^\gamma} = \text{constant}$$

is assumed to hold, where p is the pressure, ρ the density, and γ the ratio of specific heats. If the density is normalized to the value unity at infinity, and M_∞ is the Mach number at infinity, the speed of sound a is given by

$$(2.2) \quad a^2 = \frac{dp}{d\rho} = \frac{\rho^{\gamma-1}}{M_\infty^2}$$

The energy equation can then be expressed as

$$(2.3) \quad a^2 + \frac{\gamma - 1}{2} q^2 = \text{constant}$$

\mathbf{q} being the velocity vector. Also conservation of mass requires

$$(2.4) \quad \nabla \cdot (\rho \mathbf{q}) = 0$$

Since the flow is isentropic it is also irrotational. Introducing a velocity potential ϕ , the energy and mass equations can then be combined to give the transonic potential flow equation

$$(2.5) \quad \begin{aligned} (a^2 - u^2)\phi_{xx} + (a^2 - v^2)\phi_{yy} + (a^2 - w^2)\phi_{zz} \\ - 2uv\phi_{xy} - 2vw\phi_{yz} - 2uw\phi_{xz} = 0 \end{aligned}$$

in which u , v and w are the velocity components

$$(2.6) \quad u = \phi_x, \quad v = \phi_y, \quad w = \phi_z$$

The equation is elliptic at subsonic points for which $q^2 < a^2$, and hyperbolic at supersonic points for which $q^2 > a^2$.

In a weak solution for an isentropic flow the appropriate jumps to be allowed conserve mass. Thus, at a surface of discontinuity,

$$(2.7) \quad \mathbf{n} \cdot (\rho_1 \mathbf{q}_1 - \rho_2 \mathbf{q}_2) = 0$$

where \mathbf{n} is the normal to the surface, and the subscripts denote upstream and downstream conditions. At the same time the introduction of a velocity potential ensures continuity of the tangential components of velocity. Across such a jump the normal component of momentum is not conserved. The balance of momentum for the complete flow then requires a drag force on the profile equal and opposite the force on the jump. This represents the wave drag according to the isentropic approximation (cf. [11]).

The boundary condition at the boundary is

$$(2.8) \quad 0 = \mathbf{q} \cdot \boldsymbol{\nu} = \frac{\partial \phi}{\partial \boldsymbol{\nu}}$$

where $\boldsymbol{\nu}$ is the normal to the body surface. For lifting flows it is also necessary to impose the Kutta condition which requires the circulation at each section to be such that the velocity is finite at the sharp trailing edge. In the three dimensional case this results in a trailing vortex sheet across which there is a jump in potential. Using a simplified model, convection of the sheet will be ignored, and the sheet will be assumed to trail smoothly off the trailing edge without rolling up. The conditions applied at the sheet are first that the jump in potential is constant along lines in the direction of the free stream, and second that the normal velocity is continuous through the sheet. At infinity the velocity approaches a uniform far field value except near the vortex sheet. Thus $\phi \rightarrow \infty$, and it is necessary to work with a reduced potential from which the singularity at infinity has been subtracted.

3 Coordinate Systems

It is difficult to satisfy the Neumann boundary condition (2.8) with sufficient accuracy when the body surface crosses the coordinate lines. This is particularly the case near the leading edge of the wing where the surface has a high curvature and the flow is sensitive to small variations in the shape. The treatment is facilitated by the use of a curvilinear coordinate system in which the body surface coincides with a coordinate surface. In two-dimensional calculations such a system can be conveniently obtained by a conformal mapping. The potential equation (2.5) becomes

$$(3.1) \quad (a^2 - y^2)\phi_{xx} - 2uv\phi_{xy} + (a^2 - v^2)\phi_{yy} + (u^2 + v^2)(uh_x + vh_y) = 0$$

where h is the modulus of the mapping function, x and y are new coordinates in the transformed plane, and u and v are the velocity components in the new coordinate directions,

$$(3.2) \quad u = \frac{\phi_x}{h}, \quad v = \frac{\phi_y}{h}.$$

For two-dimensional flows which are subsonic at infinity, a most successful coordinate system, first introduced by Sells [12] for subcritical calculations, is obtained by a mapping of the exterior of the profile onto the interior of a circle. This coordinate system automatically bunches the mesh points in the sensitive regions near the leading and trailing edges, and has been found to give high accuracy (cf. [5], [6]). Near the center of the circle the modulus of the mapping equation approaches $\frac{1}{r^2}$ where r is the radial coordinate, and the use of finite difference formulas can lead to serious errors. It is convenient, therefore, to calculate the mapping onto the exterior of a circle and then to use an explicit inversion. If z is in the exterior of the profile and or in the exterior of the circle, then the modulus of the mapping function may be expressed as

$$h = \left| \frac{dz}{d\sigma} \right|$$

where, if ε is the included angle of the corner at the trailing edge,

$$(3.3) \quad \frac{dz}{d\sigma} = \left(1 - \frac{1}{\sigma} \right)^{1 - \frac{\varepsilon}{\pi}} \exp \left\{ \sum_{n=0}^N \frac{c_n}{\sigma^n} \right\}.$$

The mapping coefficients c_n can be calculated by a simple iterative procedure (cf. [13]). If the mapping function is to be represented at $2K$ equally spaced grid points around the circle, it is convenient to take $N = K$ so that the real and imaginary parts of the power series reduce to trigonometric interpolation formulas for functions specified at the grid points. This leads to favorable error estimates (cf. [14]). Evaluating the residue, the condition that the mapping generates a closed profile is seen to be

$$(3.4) \quad c_1 = 1 - \frac{\varepsilon}{\pi}.$$

An airfoil with a wake of constant thickness is equally easily treated. It is simply necessary to adjust the value of c_1 . If Γ is the circulation, the far field condition is (cf. [15])

$$(3.5) \quad \phi \rightarrow \frac{\cos(\theta + \alpha)}{r} + \frac{\Gamma}{2\pi} \tan^{-1}[(1 - M^2)^{1/2} \tan(\theta + \alpha)]$$

where r and θ are polar coordinates for the interior of the circle and α is the flow angle at infinity.

If the flow is supersonic at infinity the mapping to a circle is less satisfactory because we now wish to distinguish between the conditions upstream at infinity where Cauchy data is to be provided, and downstream at infinity where no condition should be imposed. A more convenient coordinate system is obtained by a mapping onto the upper half-plane. Let w denote this plane. Then this mapping is easily derived from the mapping onto the exterior of the circle by the additional transformation

$$(3.6) \quad w = \sqrt{\sigma} + \frac{1}{\sqrt{\sigma}}$$

The mapping from z to w , expressed with σ as a parameter, is then

$$(3.7) \quad \frac{dz}{dw} = \frac{dz}{d\sigma} \frac{d\sigma}{dw} = \frac{2\sqrt{\sigma}}{(1 - 1/\sigma)^{\frac{\varepsilon}{\pi}}} \exp \left\{ \sum_{n=0}^N \frac{c_n}{\sigma^n} \right\}$$

For a cusped airfoil ($\varepsilon = 0$) the singularities cancel at the trailing edge, leaving a smooth transformation. Additional stretchings of the x and y coordinates can be used to map the half-plane to a rectangle. The flow now enters the top boundary, splits, and leaves through the two sides. The airfoil covers a segment of the lower boundary. Outside this segment corresponding points have to be identified as the two sides of a cut in the z -plane, and the potential has to be continued across the cut with a jump to account for the circulation. In the far field the mapping approaches a square root transformation

$$(3.8) \quad z = w^2$$

and a suitable reduced potential which is finite at infinity is obtained by setting

$$(3.9) \quad G = \phi - (x^2 - y^2) \cos \alpha - 2xy \sin \alpha,$$

where x and y are coordinates in the transformed plane and α is the flow angle at infinity. If the flow is subsonic at infinity, the far field condition becomes

$$(3.10) \quad G = 0 \text{ on the top boundary,}$$

$$G = \pm \frac{1}{2}\Gamma \text{ on the side boundaries,}$$

where Γ is the circulation. If the flow is supersonic at infinity, it will be undisturbed upstream of the bow wave, so the condition is

$$G = 0, \quad \frac{\partial G}{\partial y} = 0 \text{ on the top boundary .}$$

An economical method of obtaining a coordinate system with similar characteristics, suggested by Garabedian, is simply to apply the square root transformation (3.8) about a point just inside the leading edge. This generates parabolic coordinates in the physical plane, while the profile is unwrapped to a bump in the transformed plane. Unfortunately it is hard to satisfy the Neumann condition with sufficient accuracy in the region of the leading edge because of the rapid variation of the mapping modulus near the singularity inside it. This difficulty can be overcome by displacing the y coordinate lines to follow the contour of the transformed profile, so that it lies on a coordinate line in a slightly nonorthogonal coordinate system (Figure 3.1). To avoid an unnecessary corner in the coordinates care should be taken to continue the cut in the physical plane smoothly off the trailing edge. It is impossible to remove the corner due to a finite wedge angle at the trailing edge, but this is a feature to be avoided in any case because it forces the appearance of a stagnation point in the inviscid flow, leading to larger adverse pressure gradients, and increasing the likelihood of boundary layer separation. The main disadvantages of a sheared parabolic coordinate system of this type are the appearance of some extra terms in the equations because the coordinates are not orthogonal, and less accurate resolution of the Kutta condition because there is no concentration of mesh points near the trailing edge.

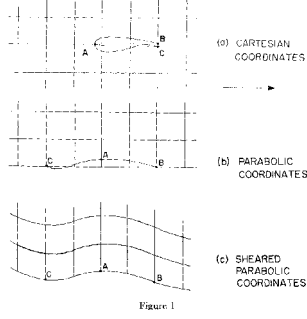


Figure 1:

In three-dimensional calculations the construction of a satisfactory coordinate system is one of the most difficult parts of the problem. For studies of an isolated wing the use of sheared parabolic coordinates appears to provide the best approach. For a tapered wing the use of a conformal transformation which varied in the spanwise direction would add numerous extra terms to the equations, and the resulting coordinate system would in any case be nonorthogonal. Under a fixed transformation independent of the spanwise coordinate, on the other hand, the potential equation retains the relatively simple form

$$(3.11) \quad \begin{aligned} & (a^2 - u^2)\phi_{xx} + (a^2 - v^2)\phi_{yy} + h^2(a^2 - w^2)\phi_{zz} \\ & - 2uv\phi_{xy} - 2hvw\phi_{yz} - 2huw\phi_{xz} + (u^2 + v^2)(uh_x + vh_y) = 0 \end{aligned}$$

Thus if the wing has a straight leading edge, which is the most usual case, the square root transformation (3.8) can conveniently be used to unwrap the sections about a singular line just inside the leading edge, so that the wing surface becomes a shallow bump above a coordinate plane formed by unfolding the two sides of a cut behind the singular line. Then, as in the two-dimensional case, the bump can be removed by displacing the coordinate surfaces so that they become parallel with the wing surface. The trailing vortex sheet is assumed to lie along the cut, so that it is also split by the transformation. A complication is caused by the continuation of the cut beyond the wing tips. Points on the two sides of the cut must be identified as representing the same physical point. Also a special form of the equations must be used at points on the ‘fold’ along the continuation of the singular line, where h vanishes. At these points the equation to be satisfied reduces to the two-dimensional Laplace equation in the x and y coordinates.

Analytical expressions for the far field potential have been given by Klunker [16]. If, however, the coordinates are stretched to infinity, the use of these can be avoided because at infinity the square root transformation collapses the region influenced by the vortex sheet to a single line of mesh points containing the sheet.

The case of a yawed wing, as proposed by R. T. Jones, is treated by keeping the coordinate system fixed to the wing, with the x, y -planes normal to the leading edge, and rotating the flow at infinity through the appropriate yaw angle, as illustrated in Figure 3.2. The vortex sheet then has to be tracked in the stream direction behind the trailing edge and downstream tip.

4 Simple and Rotated Difference Schemes

The numerical formulation of the problem requires the construction of an appropriate set of difference equations. These are then to be solved by iteration. Following the idea advanced by Murman and Cole [3], the plan of attack is to distinguish between the regions of subsonic flow, where the governing equation is elliptic, and supersonic

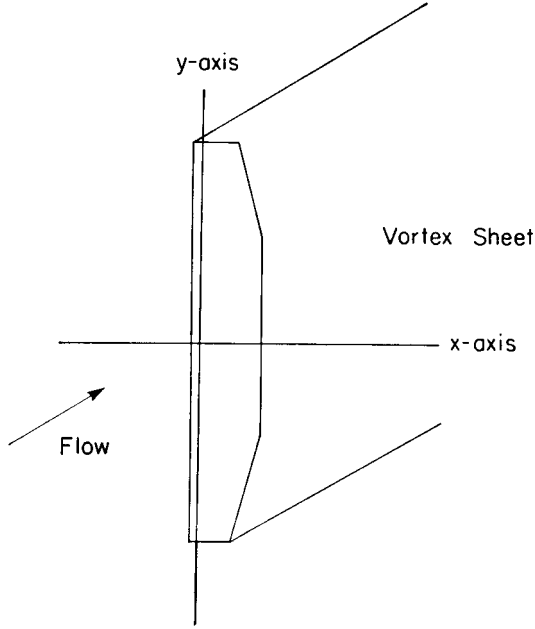


Figure 2: Yawed wing.

flow, where it is hyperbolic, and to use a difference scheme which is sensitive to the local type. For this purpose the velocities are first determined, using central difference formulas to approximate the first derivatives of the potential. Then at elliptic points central difference formulas are used for all second derivatives. At hyperbolic points streamwise second derivatives are approximated by difference formulas retarded in the upstream direction. This yields an implicit system of equations with a region of dependence which correctly reflects the region of dependence of the flow, and leads to a truncation error which has the effect of an artificial viscosity. It is important to use an implicit difference scheme, because near the sonic line the characteristics become almost perpendicular to the velocity, with the result that the mesh spacing of an explicit scheme would have to be reduced to zero in the direction of flow to obtain the correct region of dependence. The artificial viscosity ensures the desired entropy inequality, excluding expansion shocks but permitting the appearance of compression layers.

If the flow is aligned with one of the coordinates, it is relatively easy to implement these ideas. Considering the two-dimensional case (3.1) for convenience, let x be the coordinate in the flow direction. Then if the flow is supersonic at the mesh point $[i\Delta x, j\Delta y]$, we take

$$(4.1) \quad \begin{aligned} \phi_{xx} &= \frac{\phi_{ij} - 2\phi_{i-1,j} + \phi_{i-2,j}}{\Delta x^2}, \\ \phi_{xy} &= \frac{\phi_{i,j+1} - \phi_{i,j-1} - \phi_{i-1,j+1} + \phi_{i-1,j-1}}{2\Delta x \Delta y} \\ \phi_{yy} &= \frac{\phi_{i,j+1} - 2\phi_{ij} + \phi_{i,j-1}}{\Delta y^2} \end{aligned}$$

Thus we obtain a simple implicit scheme in the hyperbolic zone which can be solved line by line. The scheme is second order accurate in y and first order accurate in x . The dominant truncation errors arising from the terms in ϕ_{xx} and ϕ_{yy} are $\Delta x(u^2 - a^2)\phi_{xxx}$ and $\Delta x u v \phi_{xy}$. These represent a positive artificial viscosity

provided that $u^2 > a^2$. When the flow is not perfectly aligned with the coordinate system, there exist points in the hyperbolic region at which $u^2 < a^2 < u^2 + v^2$. These are a source of difficulty. On the one hand, a von Neumann test indicates, and experience confirms, that central difference formulas are unstable in the hyperbolic region. On the other hand, the y coordinate line now lies behind one of the characteristics from the center point $[i\Delta x, j\Delta y]$, so that use of the retarded difference formulas leads to a scheme which does not have the correct region of dependence. This is reflected in the fact that the artificial viscosity $\Delta x(u^2 a^2) \phi_{xxx}$ is now negative, and the existence of a marching instability in the x direction is confirmed by a von Neumann test.

Nevertheless, the scheme has proved extremely satisfactory in practice, provided that the supersonic flow is confined to a zone near the body in which the velocity is more or less aligned with the curvilinear coordinate system. The presence of a narrow band of points with negative numerical viscosity near the sonic line is not enough to upset the calculation. Instability can be anticipated as the mesh spacing is shrunk to zero, but more than adequate accuracy can be obtained well before its onset. Following Garabedian and Korn [5], one may also improve the accuracy by partially cancelling the truncation errors through the addition of finite difference formulas representing $\Delta x \phi_{xxx}$ and $\Delta x \phi_{xxy}$.

When the flow is supersonic at infinity, and also in three-dimensional calculations, a simple difference scheme of this type is not so satisfactory. Curvilinear coordinate systems which allow an accurate treatment of the boundary condition are generally not well aligned with the flow. We need, therefore, a coordinate invariant difference scheme. Considering first the two-dimensional case, the principal part of (3.1) can be written in the canonical form

$$(4.2) \quad (a^2 - q^2)\phi_{ss} + a^2\phi_{nn} = 0,$$

where s and n are coordinates in the local stream and normal directions. Since the direction cosines are u/q and v/q , ϕ_{ss} and ϕ_{nn} can be expressed locally in terms of the actual coordinates as

$$(4.3) \quad \begin{aligned} \phi_{ss} &= \frac{1}{q^2}(u^2\phi_{xx} + 2uv\phi_{xy} + v^2\phi_{yy}) \\ \phi_{nn} &= \frac{1}{q^2}(v^2\phi_{xx} - 2uv\phi_{xy} + u^2\phi_{yy}) \end{aligned}$$

It is now easy to devise a proper difference scheme for points in the supersonic zone. By using difference formulas retarded in both the x and y directions for all contributions to ϕ_{ss} , and central difference formulas for all contributions to ϕ_{nn} , we obtain a ‘rotated’ difference scheme which reduces to the Murman scheme when the flow is aligned with either coordinate direction. At points in the subsonic zone central difference formulas are used in the conventional manner.

A positive artificial viscosity with a magnitude proportional to $q^2 - a^2$ is introduced at all supersonic points. This enforces the correct directional property on the solution. At the same time the presence of points ahead of the y coordinate line in the formulas for ϕ_{nn} , ensures that the region of dependence of the difference scheme always contains the region of dependence of the differential equation. In the subsonic zone the scheme is second order accurate. In the supersonic zone it is second order accurate in the term representing ϕ_{nn} , but only first order accurate in the term representing $(a^2 - q^2)\phi_{ss}$, forcing the use of rather fine mesh to obtain an accurate solution.

5 Iterative Solution: Analysis Using Artificial Time

While the coordinate invariant form of the rotated difference scheme assures satisfaction of the correct entropy inequality, it also increases the difficulty of actually solving the difference equations. The use of central difference formulas in both coordinate directions for the contributions to ϕ_{nn} prevents the use of a simple marching procedure to solve the equations in the hyperbolic region a line at a time, as in the Murman scheme. Instead,

if one advances in the x direction, the correction at the point $[i\Delta x, j\Delta y]$ has to be calculated using ‘old’ values for the forward points $[(i+1)\Delta x, (j+1)\Delta y], [(i+1)\Delta x, j\Delta y]$ and $[(i+1)\Delta x, (j-1)\Delta y]$. Thus the equations in the hyperbolic region have to be solved by iteration, just as in the elliptic part of the flow.

Such a process has to be carefully controlled to ensure stability and convergence. It is helpful to regard the iterations as successive levels in an artificial time coordinate. This leads to a theory for equations of mixed type in the spirit of Garabedian’s theory for elliptic equations in [17]. The essential idea is that the iterative procedure, regarded as a finite difference scheme for a time dependent process, should be consistent with a properly posed initial value problem which is ‘compatible’ with the steady state equation; that is to say, that the solution of the initial value problem should reach an equilibrium point which represents a solution of the steady state equation. Then, if the difference scheme is also stable, it should converge to the desired solution.

Let Δt denote the time step, and let updated values of ϕ at any circle of the calculation be denoted by the superscript +. Then the typical central difference formula for a second derivative is

$$\phi_{xx} = \frac{\phi_{i-1,j}^+ - (1+r\Delta x)\phi_{ij}^+ - (1-r\Delta x)\phi_{ij} + \phi_{i+1,j}}{\Delta x^2}$$

where the updated value is used on one side, the old value on the other side because the updated value is not yet available, and a linear combination of the two is used at the center point. In the time dependent system this formula may be interpreted as representing

$$\phi_{xx} - \frac{\Delta t}{\Delta x}(\phi_{xt} + r\phi_t)$$

We must consider, therefore, a time dependent equation which contains mixed space-time derivatives. Dividing through by a^2 , its principal part will have the form

$$(5.1) \quad (M^2 - 1)\phi_{ss} + 2\alpha\phi_{st} - \phi_{nn} + 2\beta\phi_{nt} = 0$$

where M is the local Mach number q/a , and the values of α and β depend on the combination of new and old values actually used in the difference formulas. Introducing a new time coordinate,

$$(5.2) \quad T = t - \frac{\alpha s}{M^2 - 1} + \beta n$$

(5.1) becomes

$$(5.3) \quad (M^2 - 1)\phi_{ss} - \phi_{nn} - \left(\frac{\alpha^2}{M^2 - 1} - \beta^2 \right) \phi_{TT} = 0$$

If the flow is locally supersonic, it can be seen that T is spacelike and either s or n is timelike. Since s is the timelike direction in the steady state problem, we require

$$(5.4) \quad \alpha^2 > \beta^2(M^2 - 1)$$

to ensure that it is also the time-like direction in the unsteady problem. This indicates the need to add terms representing mixed space-time derivatives to the retarded difference formulas to compensate for their presence in the central difference formulas.

The characteristics of the unsteady equation (5.1) satisfy

$$(5.5) \quad (M^2 - 1)(t^2 + 2\beta nt) - 2\alpha st + (\beta s - \alpha n)^2 = 0$$

Provided that α is positive, the cone of dependence lies on the upstream side of the n,t-plane and behind the s,n-plane, touching along the line

$$n = \frac{\beta}{\alpha}s$$

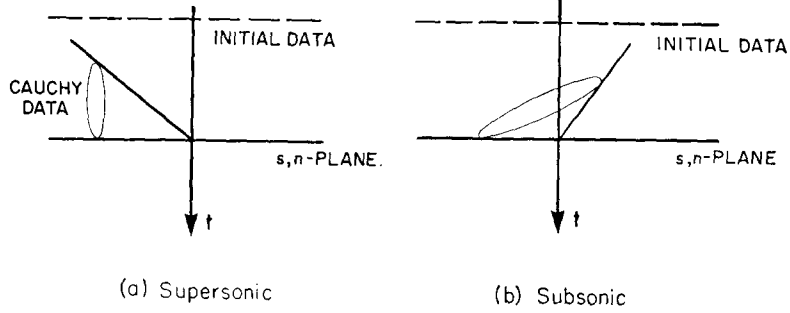


Figure 3: Characteristic cone of equivalent time dependent equation.

as illustrated in Figure 5.1. Thus the region of dependence at the current time level is reduced to a single line, and an iterative scheme with the correct region of dependence can be obtained simply by ensuring that the points surrounding this line have already been updated. If α is negative, the cone of dependence is in the downstream direction. Thus to ensure the proper region of dependence it is necessary to control both the magnitude and the sign of the coefficient of ϕ_{st}

A von Neumann test of local stability leads to an additional guideline. Let the differential equation be approximated at the mesh point $[i\Delta x, j\Delta y]$ by the general difference equation

$$\sum_{p,q} (a_{pq}\phi_{i+p,j+q} - b_{pq}\phi_{i+p,j+q}^+) = 0$$

Substituting the formula

$$\phi = G^k e^{imx} e^{iny}$$

for ϕ at the k-th time interval, the growth factor G is given by

$$G = \frac{\sum_{p,q} a_{pq} e^{i(p\xi + q\eta)}}{\sum_{p,q} b_{pq} e^{i(p\xi_q \eta)}}$$

where

$$\xi = m\Delta x, \quad \eta = n\Delta y.$$

For small values of ξ and η , G may be expanded as

$$G = \frac{A_{00} + A_{10}i\xi + A_{01}in + A_{20}\xi^2 + A_{11}\xi\eta + A_{02}\eta^2 + \dots}{B_{00} + B_{10}i\xi + B_{01}in + B_{20}\xi^2 + B_{11}\xi\eta + B_{02}\eta^2 + \dots}$$

where consistency with the steady state differential equation (3.1) requires that

$$A_{00} = B_{00}, \quad A_{10} = B_{10}, \quad A_{01} = B_{01},$$

$$B_{20} - A_{20} = \frac{a^2 - u^2}{\Delta x^2}, \quad B_{11} - A_{11} = \frac{-2uv}{\Delta x \Delta y}, \quad B_{02} - A_{02} = \frac{a^2 - v^2}{\Delta y^2}$$

Since ξ and η can be chosen so that

$$(a^2 - u^2) \frac{\xi^2}{\Delta x^2} - 2 \frac{2uv\xi\eta}{\Delta x \Delta y} + (a^2 - v^2) \frac{\eta^2}{\Delta y^2}$$

is either positive or negative, whenever the flow is supersonic, $|G|$ can certainly exceed unity unless

$$A_{00} = B_{00} = 0$$

It follows that

$$\sum_{p,q} a_{pq} = \sum_{p,q} b_{pq} = 0$$

Interpreting the difference scheme as the representation of a time-dependent process, this means that the coefficient of ϕ_t should be zero at supersonic points, reflecting the fact that t is not a time-like direction. This is in contrast to the subsonic part of the flow. There the damping due to ϕ_t , plays a critical role in the convergence of the successive overrelaxation process for an elliptic equation (cf. [16]). The mechanism of convergence in the supersonic zone can be inferred from Figure 5.1. An equation of the form (5.1) with constant coefficients reaches a steady state because with advancing time its characteristic cone (5.5) eventually ceases to intersect the initial time-plane. Instead it intersects a surface containing the Cauchy data of the steady state problem. The rate of convergence is determined by the backward inclination of the most retarded characteristic

$$t = \frac{2\alpha s}{M^2 - 1}, \quad n = -\frac{\beta}{\alpha} s,$$

and is maximized by using the smallest permissible coefficient α for the term in ϕ_{st} . In the subsonic zone, on the other hand, the cone of dependence contains the t -axis, and it is important to introduce damping to remove the influence of the initial data.

It is possible to devise both point and line relaxation schemes based on these principles. Line relaxation is generally preferable because it spreads the influence of the boundaries and the effects due to circulation faster, and gives more latitude in ensuring that the region of dependence is correct. The following is a line relaxation algorithm which has proved effective. First derivatives are represented throughout the flow by central difference formulas using values frozen from the previous cycle:

$$(5.6) \quad \phi_x = \frac{\phi_{i+1,j} - \phi_{i-1,j}}{2\Delta x}, \quad \phi_y = \frac{\phi_{i,j+1} - \phi_{i,j-1}}{2\Delta y}$$

Velocities computed from the first derivatives are used to determine whether the point is elliptic ($q^2 < a^2$) or hyperbolic ($q^2 > a^2$). At hyperbolic points the principal part of the equation is written in the canonical form (4.2). If the values of ϕ on a y coordinate line are to be updated, the contributions to ϕ_{nn} are represented by the central difference formulas

$$(5.7) \quad \begin{aligned} \phi_{xx} &= \frac{\phi_{i-1,j}^+ - \phi_{ij}^+ - \phi_{ij} + \phi_{i+1,j}}{\Delta x^2} \\ \phi_{xy} &= \frac{\phi_{i-1,j-1}^+ - \phi_{i-1,j+1}^+ - \phi_{i+1,j-1} + \phi_{i+1,j+1}}{4\Delta x \Delta y} \\ \phi_{yy} &= \frac{\phi_{i,j+1}^+ - 2\phi_{ij}^+ - \phi_{i,j-1}^+}{\Delta y^2} \end{aligned}$$

where the superscript + has again been used to denote updated values. These formulas add a contribution

$$\frac{v}{q} \frac{\Delta t}{\Delta x} \phi_{nt}$$

to the equivalent time dependent equation (5.1). The contributions to ϕ_{ss} are represented by retarded difference formulas evaluated from the ‘upstream’ quadrant containing the reversed velocity vector. If $u > 0, v > 0$, we take

$$(5.8) \quad \phi_{xx} = \frac{2\phi_{ij}^+ - \phi_{ij} - 2\phi_{i-1,j}^+ + \phi_{i-2,j}}{\Delta x^2}$$

$$\phi_{xy} = \frac{2\phi_{ij}^+ - \phi_{ij} - \phi_{i-1,j}^+ + \phi_{i,j-1}^+ + \phi_{i-1,j-1}}{\Delta x \Delta y}$$

$$\phi_{yy} = \frac{2\phi_{i,j}^+ - \phi_{ij} - 2\phi_{i,j-1}^+ + \phi_{i,j-2}}{\Delta y^2}$$

These formulas produce a contribution

$$2(M^2 - 1) \left(\frac{u}{q} \frac{\Delta t}{\Delta x} + \frac{v}{q} \frac{\Delta t}{\Delta y} \right) \phi_{st}$$

to compensate for the term in ϕ_{nt} . They also lead to a diagonally dominant tridiagonal set of equations for the new values ϕ^+ on each line, which are easy to solve. Near the sonic line, where $M^2 - 1$ approaches zero, the term in ϕ_{st} , should be augmented to satisfy condition (5.4). A suitable stabilizing term is

$$\epsilon \left(\frac{\Delta t}{\Delta x} \left(\frac{u}{q} \right) \phi_{xt} + \frac{\Delta t}{\Delta y} \left(\frac{v}{q} \right) \phi_{yt} \right)$$

where ϵ is a parameter which must be chosen to be sufficiently large. If $u > 0, v > 0$, then ϕ_{xt} and ϕ_{yt} are represented as

$$(5.9) \quad \begin{aligned} \phi_{xt} &= \frac{\phi_{ij}^+ - \phi_{ij} - \phi_{i-1,j}^+ + \phi_{i-1,j}}{\Delta t \Delta x} \\ \phi_{yt} &= \frac{\phi_{ij}^+ - \phi_{ij} - \phi_{i,j-1}^+ + \phi_{i,j-1}}{\Delta t \Delta y} \end{aligned}$$

These formulas preserve the diagonally dominant tridiagonal form of the line equations. In practice it often proves possible to take $\epsilon = 0$.

At subsonic points all terms are represented by the same central difference formulas that are used for the contributions to ϕ_{nn} , except that ϕ_{xx} is represented as

$$(5.10) \quad \phi_{xx} = \frac{\phi_{i-1,j}^+ - \frac{2}{\omega} \phi_{ij}^+ - 2 \left(1 - \frac{1}{\omega} \right) \phi_{ij} + \phi_{i+1,j}}{\Delta x^2}$$

where ω is the over-relaxation factor with a value between 1 and 2. This is an adjustment to the usual formulation of successive over-relaxation. It preserves continuity of the representation of ϕ_{yy} between points where the type changes, so that the optimal value of w can be used throughout the elliptic region without creating a disturbance at the sonic line.

6 Three-Dimensional Difference Scheme

The same ideas are easily extended to the three-dimensional case. The principal part of governing equation (3.11) is written in the canonical form

$$(6.1) \quad (a^2 - q^2) \phi_{ss} + a^2 (\Delta \phi - \phi_{ss}) = 0$$

where Δ is the Laplacian

$$(6.2) \quad \Delta \phi = \phi_{xx} + \phi_{yy} + h^2 \phi_{zz}$$

and

$$(6.3) \quad \begin{aligned} \phi_{ss} = & \frac{1}{q^2} (u^2 \phi_{xx} + v^2 \phi_{yy} + h^2 w^2 \phi_{zz} \\ & + 2uv\phi_{xy} + 2hvw\phi_{yz} + 2huw\phi_{xz}) \end{aligned}$$

Then, as before, ϕ_{ss} is represented by retarded difference formulas and $\Delta\phi - \phi_{ss}$ by central difference formulas at all hyperbolic points, with care taken to make sure that the equivalent time-dependent equation contains a large enough coefficient for ϕ_{st} and a zero coefficient for ϕ_t . The formulation in terms of the Laplacian eliminates the need to determine explicitly a pair of local coordinate directions in the plane normal to the stream direction.

It is convenient to solve the equations a line at a time, corresponding to a point relaxation process in two dimensions. Any of the coordinate lines may be used for this purpose, the choice being guided by the need to avoid advancing through the hyperbolic region in a direction opposed to the flow. This constraint is dictated by the split between new and old values in the retarded difference formulas which are used to represent ϕ_{ss} and the added term in ϕ_t . In practice it has been found convenient to divide each x,y-plane into three strips, and to march towards the surface in the central strip, updating horizontal lines, and then outwards in the left-hand and right-hand strips, updating vertical lines.

7 Boundary Conditions and Kutta Condition

The Neumann boundary condition (2.8) is satisfied by introducing a row of dummy points behind the boundary. The potential at each dummy point is given a value such that the normal velocity at the surface computed from a central difference formula is zero. The flow equations are then represented at the surface by the standard difference formulas. Thus the boundary condition is satisfied with second order accuracy, while the flow equations are satisfied with the same accuracy as at interior points. In the iterative solution procedure the values of the potential at the dummy points are updated to satisfy the boundary condition in the course of each cycle.

In calculations with lift the circulation has to be adjusted to satisfy the Kutta condition. In two-dimensional calculations this requires only a minor complication. Along a cut behind the trailing edge there should be a constant jump Γ in the circulation. In the circle plane this is easily accommodated by subtracting a term $\Gamma\theta/2\pi$ from the potential and writing difference equations for the resulting single-valued function G . At the trailing edge the modulus of the mapping function is zero. Then the velocity computed according to formula (3.2) would be infinite unless

$$\phi_\theta = G_\theta - \frac{\Gamma}{2\pi} = 0$$

Γ is therefore updated at the end of each cycle, so that this condition is satisfied when G_θ is represented by a central difference formula.

In calculations using either a conformal mapping or a sheared square root transformation to the half-plane, the cut is opened up to form part of the lower boundary (Figure 3.1). As in the treatment of the boundary condition on the profile, dummy points are introduced below the boundary. These may be identified with corresponding interior points, obtained by reflection about the origin, which map to the same points in the physical plane. The potential at each dummy point is therefore set to the value at the corresponding interior point augmented by the jump $\pm\Gamma$. Each point along the boundary on one side of the cut is treated as an interior point, using the standard difference equations, and the potential at the corresponding point on the other side of the cut is set by adding the value of the jump.

In three-dimensional calculations a similar procedure is employed. Since, however, the cut now represents the vortex sheet, it is no longer appropriate to satisfy the flow equations at the boundary points. Instead the condition that the vertical component of velocity is continuous through the vortex sheet is represented by equating the corresponding finite difference expressions for ϕ_y , on the two sides of the sheet. The value of the

jump at each point on the sheet is assigned the value at the corresponding point on the trailing edge, obtained by projection in the direction of the undisturbed stream.

8 Computations

The proposed relaxation procedure has been programmed in FORTRAN for both two- and three-dimensional flows. Calculations are normally performed on several meshes. A solution is first obtained on a coarse mesh, and the result is interpolated to provide the initial guess for a calculation in which the mesh spacing is halved in each coordinate direction by the introduction of new mesh points. This process may be repeated. When the mesh spacing is halved, the rate of convergence is also roughly halved because the effective time step is proportional to the mesh spacing. Allowing for the increase in the number of mesh points, the computer time required to reach a solution from a given initial estimate can therefore be expected to increase roughly by a factor of eight in two-dimensional calculations, or sixteen in three-dimensional calculations. The procedure of mesh refinement thus leads to significant savings of computer time by providing good starting guesses for the fine mesh calculations. It also serves the purpose of providing an indication of the convergence of the solution of the difference equations to the solution of the differential equations.

Numerous flow computations have been performed with the aid of the CDC 6600 belonging to the AEC Computing and Applied Mathematics Center at New York University. Some of these have been for the purpose of generating data for a forthcoming second volume on supercritical wing sections [18]. Provided that the mesh refinement procedure is used, a sufficiently accurate answer can generally be obtained after 100 to 200 cycles on the fine mesh. Typically a two-dimensional calculation with a fine mesh of 6144 cells takes about 5 minutes, and a three-dimensional calculation with a fine mesh of 98304 cells takes about 45 minutes.

The merits of mappings to the circle and half-plane have been tested in two-dimensional calculations. The Kutta condition is less accurately treated in the coordinate systems which use a mapping to the half-plane, either by a conformal transformation or the introduction of sheared parabolic coordinates. Nevertheless the results remain very satisfactory, confirming the suitability of these systems for the extensions to supersonic free streams and three-dimensional flows. All the presented results were obtained using the sheared parabolic coordinate system.

Figures 8.1 and 8.2 display some results from a study over a wide Mach range of an airfoil designed by Garabedian to produce very high lift with shock free flow. Figure 8.1 shows the pressure distribution near the design condition, and also at Mach 1. Figure 8.2 shows the computed drag rise and loss of lift through Mach 1. This result is in accord with the general experience of wind tunnel and flight tests, although in practice the strong shock waves which occur after the onset of drag rise would lead to separated flow.

No difficulties have been encountered in calculating flows with a free stream at exactly Mach 1. The pattern of the flow near the wing remains essentially unaltered as the Mach number at infinity is increased beyond one, while a weak bow wave appears far upstream. Near Mach 1 the calculations usually indicate a ‘fish tail’ shock pattern at the trailing edge, as sketched in Figure 8.3. Such patterns have been experimentally observed, but whereas the calculations show strong oblique shocks at the trailing edge, with a subsonic zone in the fish tail, the experiments show weak oblique shocks through which the flow remains supersonic.

In order to test the stability and accuracy of the three-dimensional difference scheme, a number of calculations have been performed for an infinite yawed wing. The conditions for simple sweepback theory are then exactly satisfied. If the Mach number normal to the leading edge is fixed while the yaw angle is varied, we expect the solution to consist of an invariant flow in the plane containing the wing section together with a uniform superposed spanwise velocity. The flow is seen differently by the difference scheme, however, because the number of supersonic points increases as the yaw angle and corresponding total Mach number are increased. It was

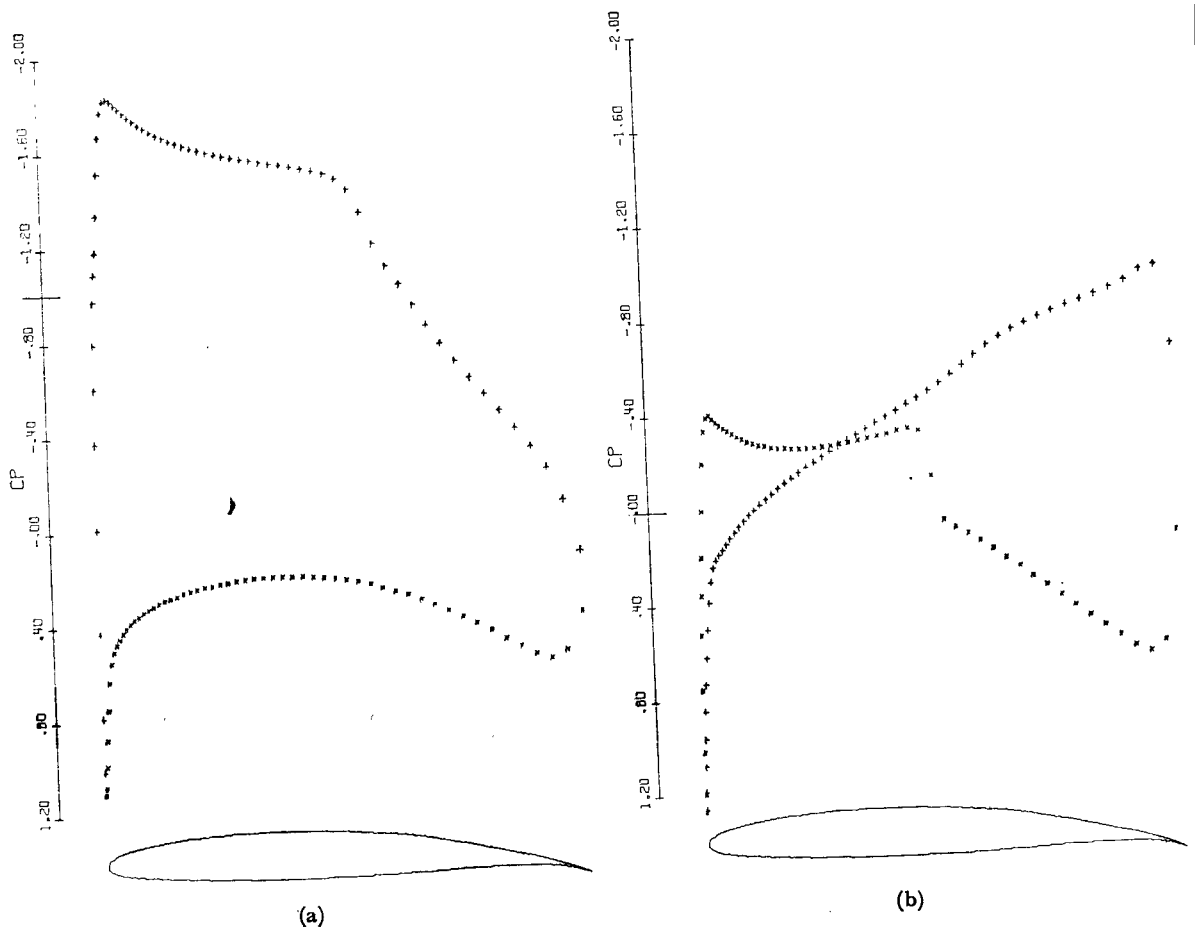


Figure 4: (a) At Mach 0.65, Angle of attack 0° , Lift coefficient 1.4930, Drag coefficient -0.0005 (b) At Mach 1, Angle of attack 0° , Lift coefficient 0.5048, Drag coefficient 0.1154

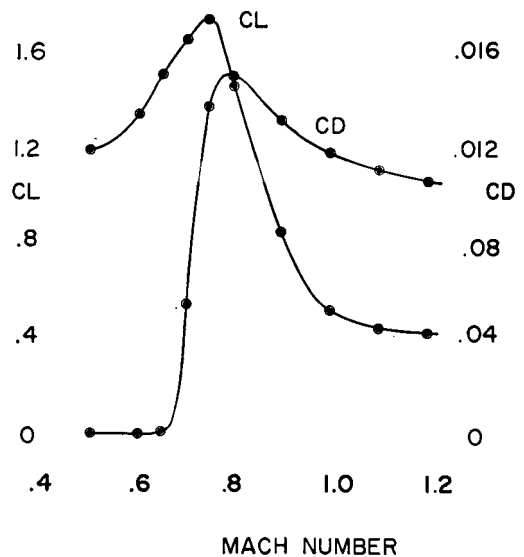


Figure 5: Lift and drag of 65-15-10 airfoil.

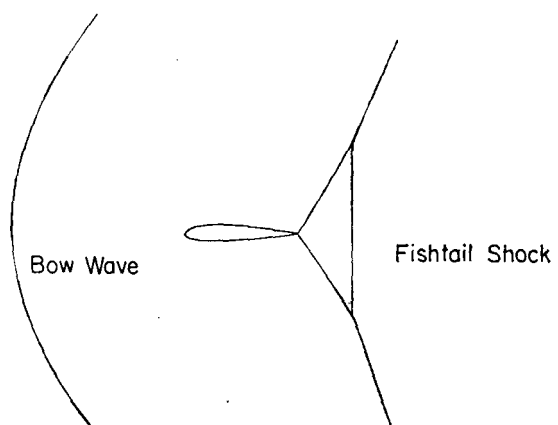


Figure 6: Shock pattern near Mach 1.

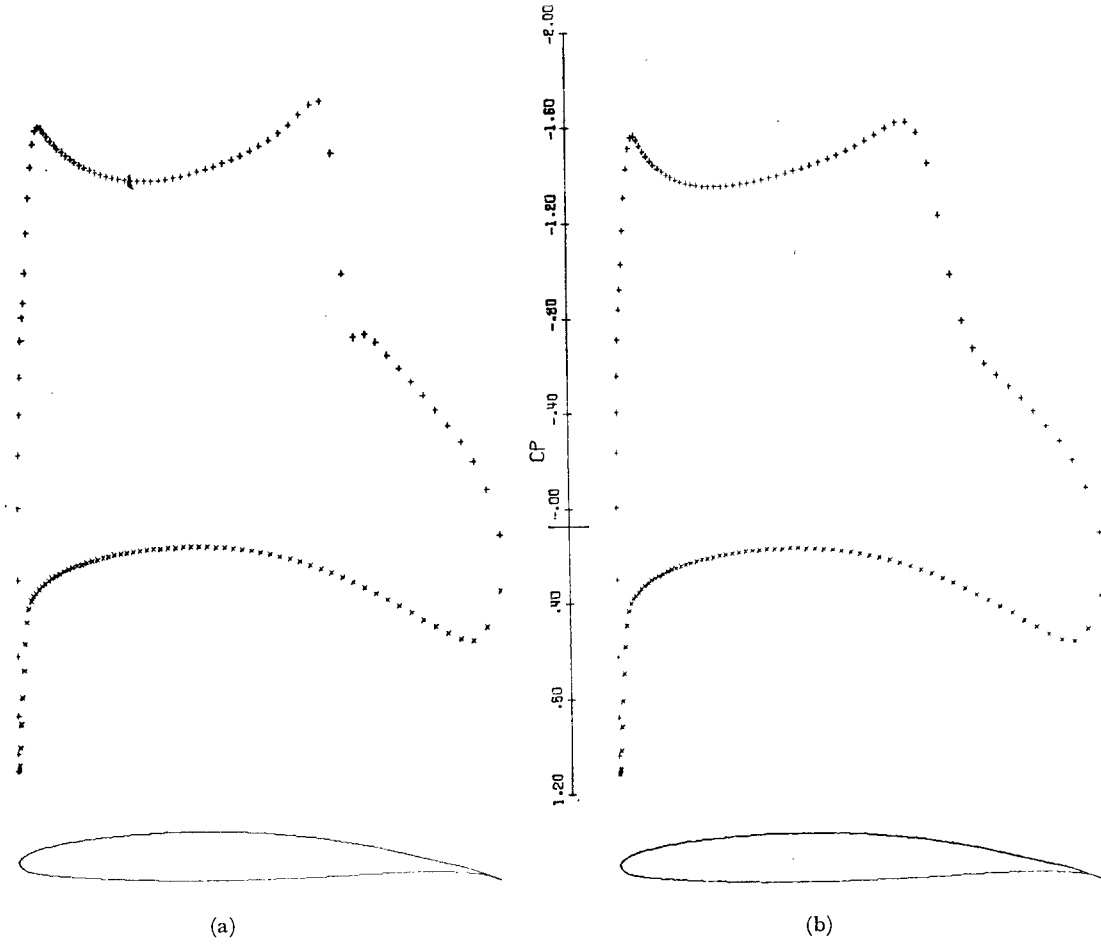


Figure 7: (a) Unyawed at Mach 0.67, Angle of attack -0.5° , Lift coefficient 1.4249, Drag coefficient 0.0074 (b) Yawed 48.9° at Mach 1.02, Angle of attack -0.5° , Lift coefficient 1.4242, Drag coefficient 0.0093

verified that the computed solutions do have the expected invariance, as illustrated in Figure 8.4. If the flow is supersonic behind a shock wave, however, the shock is less sharply represented, being spread over 4 to 5 mesh widths.

Figures 8.5 and 8.6 display results of three-dimensional calculations for wings of finite aspect ratio. Figure 8.4 shows an unyawed wing at Mach 0.82 and an angle of attack of 1° . The central panel has a section designed by Garabedian for a lift coefficient of 0.6 at Mach 0.78. Over each outer panel the section is gradually altered to a less highly cambered profile at the tip. The pressure distributions at successive span stations are plotted above each other at equal vertical intervals. It can be seen that there is a transition from a single shock wave at the center to a multiple shock pattern near the tip, with almost shock-free flow in between. Figure 8.6 shows a similar wing at Mach 1, yawed through 36° , and with some twist introduced to equalize the load across the span. The leading tip is at the bottom and the trailing tip is at the top of the picture. The shock waves are now smudged, but their accumulation towards the trailing tip is evident.

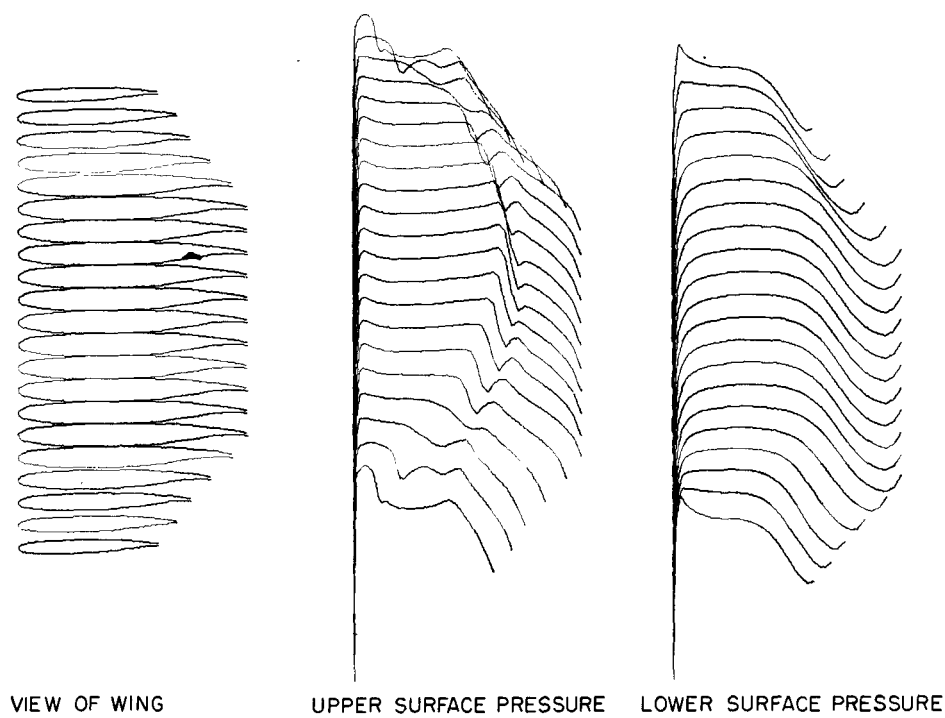


Figure 8: Angle of attack 1.8° , Unyawed wing at Mach 0.82, Lift coefficient 0.5139, Lift drag ratio 22.05, Drag coefficient 0.0233

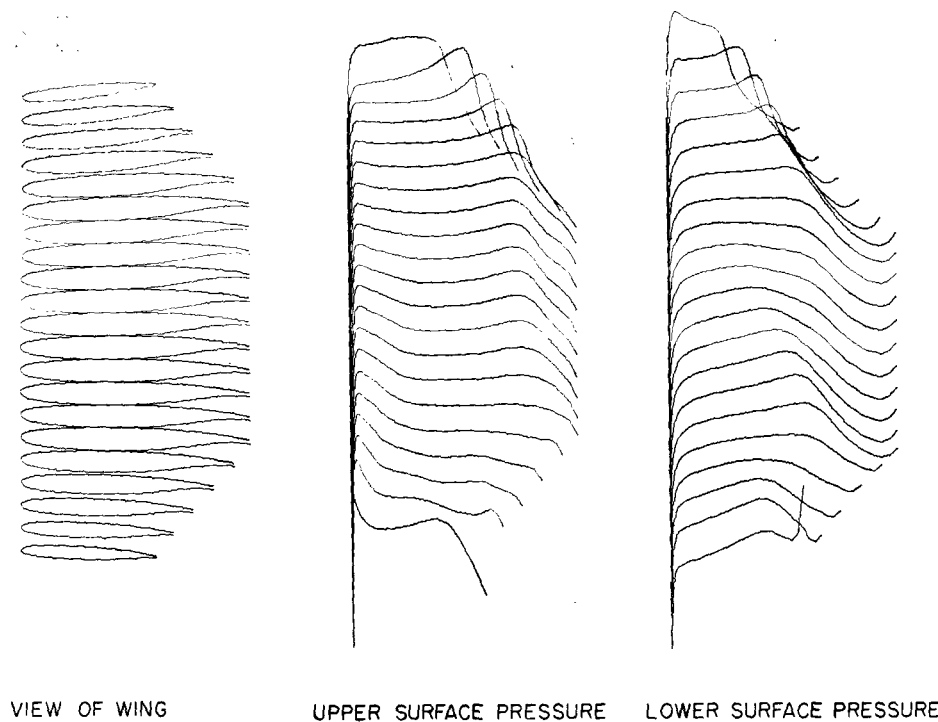


Figure 9: Wing yawed 36° at Mach 1 with trailing tip at the top, Angle of attack 1.8° , Lift coefficient 0.2327, Drag coefficient 0.0201, Lift drag ratio 11.59

9 Conclusion

The results of these computations reinforce the view that the computer can eventually be used as a ‘numerical wind tunnel’. The repeated and reliable convergence of the method at all Mach numbers, including Mach I, provides numerical confirmation of the existence and uniqueness of weak solutions of the potential equation when a suitable entropy inequality is enforced. The method achieves speed and economy by simulating an artificial time dependent equation constructed so that it will reach a steady state as fast as possible. This is in contrast to the proposal to integrate the physical time dependent equation of an unsteady flow (cf. [19]), a method which has been found to converge slowly to the steady state.

In order to improve the treatment of shock waves it would be desirable to introduce a shock fitting procedure to enforce more precisely the jump condition (2.7), rather than rely on the artificial viscosity introduced by the difference scheme to generate the correct jumps. A more accurate representation of shock waves might also be obtained by using the divergence form (2.4) of the potential equation, and making sure that the artificial viscosity introduced by backward difference operators was also in conservative form, as in Murman’s latest scheme for the small disturbance equations (cf. [20]).

The other main disadvantage of the present scheme is its use of first order accurate difference equations in the hyperbolic region. When the flow is mainly subsonic, with a small embedded supersonic zone, it is easy to compensate for this by bunching the mesh points near the body. When the flow is supersonic at infinity it forces the use of a large number of mesh points to obtain an accurate answer. An equation resembling the flutter equation

$$\phi_{tt} + 2u\phi_{xt} + 2v\phi_{yt} = (a^2 - u^2)\phi_{xx} - 2uv\phi_{xy} + (a^2 - v^2)\phi_{yy}$$

would be obtained by the addition of an explicit term in ϕ_{tt} . This would require a three level difference scheme, but would have the advantage of rotating the cone of dependence fully behind the current time level, allowing more latitude for the construction of a scheme with a higher order of accuracy.

References

- [1] Jones, R. T., *Reduction of wave drag by antisymmetric arrangement of wings and bodies*, AIAA Journal, Vol. 10, 1972, pp. 171-176.
- [2] Bauer, F., Garabedian, P., and Korn, D., *Supercritical Wing Sections*, Springer-Verlag, New York, 1972.
- [3] Murman, E. M., and Cole, J. D., *Calculation of plane steady transonic flows*, AIAA Journal, Vol. 9, 1971, pp. 114-121.
- [4] Steger, J. L., and Lomax, H., *Transonic flow about two-dimensional airfoils by relaxation procedures*, AIAA Journal, Vol. 10, 1972, pp. 49-54.
- [5] Garabedian, P. R., and Korn, D., *Analysis of transonic airfoils*, Comm. Pure Appl. Math., Vol. 24, 1972, pp. 841-851.
- [6] Jameson, Antony, *Transonic flow calculations for airfoils and bodies of revolution*, Grumman Aerodynamics Report 390-71-1, December 1971.
- [7] Bailey, F. R., and Ballhouse, W. F., *Relaxation methods for transonic flow about wing-cylinder combinations and lifting swept wings*, Third International Conference on Numerical Methods in Fluid Dynamics, Paris, July 1972.
- [8] Morawetz, C. S., *On the non-existence of continuous transonic flows past profiles*, Comm. Pure Appl. Math., Vol. 9, 1956, pp. 45-68.

- [9] Lax, Peter D., *Weak solutions of nonlinear hyperbolic equations and their numerical computation*, Comm. Pure Appl. Math., Vol. 7, 1954, pp. 159-193.
- [10] Hayes, Wallace D., *The basic theory of gas dynamic discontinuities*, Section D, *Fundamentals of Gas Dynamics*, edited by Howard W. Emmons, Princeton, 1958.
- [11] Steger, J. L., and Baldwin, B. S., *Shock waves and drag in the numerical calculation of isentropic transonic flow*, NASA TN D-6997, 1972.
- [12] Sells, C. C. L., *Plane subcritical flow past a lifting airfoil*, Proc. Roy. Soc. London, Vol. 308A, 1968, pp. 377-401.
- [13] James, R. M., *A new look at incompressible airfoil theory*, McDonnell Douglas Report j 0198, May 1971.
- [14] Snider, Arthur D., *An improved estimate of the accuracy of trigonometric interpolation*, SIAM J. Num. Analysis, Vol. 9, 1972, pp. 505-508.
- [15] Ludford, G. S. S., *The behavior at infinity of the potential function of a two-dimensional subsonic compressible flow*, J. Maths. Phys. Vol. 30, 1951, pp. 131-159.
- [16] Klunker, E. B., *Contribution to methods for calculating the flow about thin lifting wings at transonic speeds analytic expressions for the far field*, NASA TN D6530, 1971.
- [17] Garabedian, P. R., *Estimation of the relaxation factor for small mesh size*, Math. Tables Aids Comp., Vol. 10, 1956, pp. 183-185.
- [18] Bauer, F., Garabedian, P., Jameson, A., and Korn, D., *Supercritical wing sections 2*, NASA SP, to appear.
- [19] Magnus, R., and Yoshihara, H., *Inviscid transonic flow over airfoils*, AIAA Journal, Vol. 8, 1970, pp. 2157-2162.
- [20] Murman, Earll M., *Analysis of embedded shock waves calculated by relaxation methods*, AIAA Computational Fluid Dynamics Conference, Palm Springs, California, July 1973.